Available online at www.CivileJournal.org

Civil Engineering Journal

(E-ISSN: 2476-3055; ISSN: 2676-6957)

Vol. 11, No. 12, December, 2025

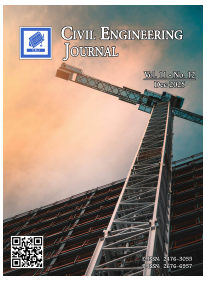

Effect of Air Pressure on Changes in Parameters and Soil Settlement Behavior in Very Soft Soils

Encu Sutarman [1, 2*], Sri Prabandiyani Retno Wardani [1], Agus Setyo Muntohar [3]

[1] Department of Civil Engineering, Faculty of Engineering, Diponegoro University, Semarang 50241, Indonesia.

[2] Lecturer in Geotechnics at the Department of Civil Engineering, Faculty of Engineering, Langlangbuana University, Bandung 40261, Indonesia.

[3] Department of Civil Engineering, Faculty of Engineering, Muhammadyah University Yogyakarta, Jogjakarta 55183, Indonesia.

Received 30 April 2025; Revised 24 October 2025; Accepted 06 November 2025; Published 01 December 2025

Abstract

An effective soil improvement method is essential in soft soil due to the poor bearing capacity for construction loads. To address the challenge, the use of the staged air pressure method with Suction Assisted Vacuum Preloading (SAVP) has shown significant potential when applied through Geosystem Air Booster Vacuum Preloading (GAVP), specifically designed with a sensor system as a real-time measuring tool for soil parameter changes. Therefore, this research aims to examine the effectiveness of the SAVP method in relation to the discharge of drained water from prefabricated vertical drains (PVD) on changes in soil parameters due to air pressure and vacuum using the GAVP tool. The method used five PVDs in large-diameter soil sample tubes, applying air pressure and vacuum simultaneously and selectively. This experimental setup was designed to examine the fundamental aspects of soil parameter changes, namely permeability, consolidation, and volume compression coefficient. The results showed that soil parameters during testing interacted with each other, where air pressure balanced with vacuum caused changes and optimized settlement and consolidation efficiency. Decreasing air pressure enhanced vacuum performance, causing a corresponding rise in soil settlement and consolidation degree. However, increasing air pressure decreased soil settlement and the degree of consolidation.

Keywords: Consolidation; Soft Soil Parameters; Vacuum Preloading; Air Pressure.

1. Introduction

The Conventional Vacuum Preloading (CVP) method is widely used for soft soil improvement. This method is effective [1] and provides good soil results [2]. However, there are several shortcomings associated with CVP, namely a large loss of vacuum strength, additional loads, drainage blockage from prefabricated vertical drains (PVD), soil improvement only in shallow layers [3], and inaccurate groundwater level monitoring [4]. To address these challenges, numerous methods have been developed, such as vacuum preloading [4–13], surcharge preloading [14], and Air Booster Vacuum Preloading (AVP) [12, 15–26]. The vacuum preloading method is a combination of vacuum and PVD used in the field for soft soil improvement [2, 6, 11, 27]. However, the effect of vacuum transfer causes unevenness in soil surface settlement [28]. Previous research has shown that using vacuum preloading without sand, combined with short and long PVD (VPSL), is more effective than the CVP method in improving the top layer of soft soil to achieve uniform strength [29]. Vacuum preloading can also reduce consolidation time [30] and obtain information about soft soil deformation [31]. The main disadvantage of this method is the blockage of PVD drainage, which causes a decrease in

* Corresponding author: encu_sutarman@unla.ac.id

http://dx.doi.org/10.28991/CEJ-2025-011-12-020

© 2025 by the authors. Licensee C.E.J, Tehran, Iran. This article is an open access article distributed under the terms and conditions of the Creative Commons Attribution (CC-BY) license (http://creativecommons.org/licenses/by/4.0/).

vacuum and drainage capacity [32, 33]. To address this disadvantage, the Step Vacuum Preloading (SVP) method has proven effective [13, 34–37], but still causes lateral soil displacement inward [13].

Surcharge preloading is another widely used method, which combines PVD with an additional load for soft soil improvement [38]. However, this method causes lateral soil displacement outward, which can be minimized by combining vacuum and surcharge preloading. The combination of air pressure and vacuum preloading (AVP) is also used due to a faster effect [15]. The air pipe in the AVP method is placed under the soft soil layer, creating a pressure difference that causes cracks in the soil, thereby accelerating drainage from the PVD and contributing to consolidation [12]. Previous research has compared AVP and CVP in the laboratory using an electron microscope and mercury intrusion porosimetry to obtain the difference between both methods in accelerating consolidation [18]. The AVP method, which includes laboratory testing of the position and type of air pipe for very soft soil samples, was used to examine the vertical pressure effect at the middle and bottom of the soil layer [16]. Further analysis investigated how the duration of air pressure influenced pore water pressure and vacuum. The results showed extremely short duration caused insufficient pore water pressure dissipation to achieve the desired effect. However, a longer duration led to excessive air entrapment in soil, causing a decrease in vacuum [17]. Research was also conducted on the effect of air pressure duration on soil permeability due to pressure between PVD at the injection point. The results showed that longer duration caused small cracks, increasing permeability and decreasing vacuum [19].

Testing the consolidation behavior of homogeneous multilayers using the AVP method found that the consolidation theory is not yet perfect and only focuses on the reinforcement mechanism of one layer of soil [20]. Conventional vacuum preloading is prone to clogging in PVD filters and requires additional loading in the form of large sand deposits, whereas the AVP method has been developed to overcome this clogging but still requires more data to verify its performance [21]. Laboratory tests of air-boosted vacuum consolidation on dredged soil slurry found that compressed air induces cracks in the soil, accelerating the drainage consolidation of dredged soil slurry [22]. Air boosters provided in an alternating pattern alongside PVD can increase pore pressure and open blocked soil pores [23]. Analytical consolidation using the AVP method combining vacuum attenuation and air pressure, the results of parametric sensitivity analysis revealed a significant correlation between consolidation efficiency when compared with the conventional model, where an increase in the consolidation rate was observed with a higher vacuum load coefficient and an increased Poisson's ratio [24]. The vacuum preloading and hot air pressure method by injecting hot gas—the test results showed that the pore water pressure increased and the soil gradually rebounded so that the soil crack gap was reduced during the heating process [25]. The AVP method with the addition of polyacrylamide to the dredged mud increase can improve consolidation efficiency by increasing the hydraulic gradient and inducing fractures in the soil, encouraging the aggregation of fine soil particles, reducing drainage channel blockage through adsorption, and increasing vacuum transmission, but excessive addition of polyacrylamide and high air pressure can interfere with the effectiveness of vacuum preloading performance [26].

The AVP method uses vacuum and air pressure as preloading by applying the duration and magnitude of air pressure in a single testing period. In this method, PVD serves as the primary channel for water drainage, while air pressure is applied through flexible pipes. However, a significant limitation of flexible pipes is their unsuitability for large-scale soil improvement in the field, even after modifications. Laboratory testing of the AVP method includes a soil sample tube, often equipped with an electron microscope and mercury intrusion porosimetry. Some setups also use sensors as monitoring tools connected to a monitor. During testing, several variables are monitored, including vacuum pressure, soil settlement, water discharge, and pore water pressure. This is followed by measurements of water content and shear strength of the soil.

According to Lei et al. [18], the AVP method offers several benefits, including the ability to reduce PVD drainage blockage, effectiveness, and a relatively short construction period. This method has disadvantages, such as the use of conventional flexible air pipes limiting insertion depth; air pipe insertion is limited, which prevents application for improving deeper layers of soft soil [18]. Although factors like soil settlement, PVD drainage rate, water content, pore water pressure, and soil shear strength affect each other during preloading, their correlation with changes in various soft soil properties has not been fully analyzed [37]. This shows the need for further investigation focusing on the combination of air pressure with vacuum preloading, specifically using the SAVP method. Therefore, this research aimed to examine the impact of air pressure on PVD water discharge, changes in soft soil parameters, soil settlement, and consolidation using the SAVP method. The problems addressed in this research included the effect of air booster pressure on the discharge of drained water from PVD, changes in the characteristics of very soft soil, and the relationship between parameters during preloading work, as well as soil settlement and consolidation.

The novelty of this research is the real-time measurement of changes in air pressure, vacuum preloading, pore water pressure, preloading combination pressure, soil settlement, groundwater subsidence, and drained water discharge from

PVD. Analysis is also carried out to examine the effect of water discharge on changes in soft soil parameters such as soil permeability, consolidation coefficient, and volume compression coefficient. Additionally, the relationships between these parameters are evaluated to derive equations for soil parameters related to water discharge. The results are expected to provide benefits for geotechnical science, soft soil improvement construction service operators, and the government, which serves as both a regulator and employer of infrastructure, such as toll roads, very soft soil dredging, and others.

2. Method

The SAVP method used vacuum and air booster pressure as preloading by gradually applying the active period, allowing for real-time observation of air pressure on changes in soft soil parameters. In this research, a laboratory model test was conducted. The model consisted of soil tank (see Figure 1) which was equipped with electronic sensors for measuring pore water pressure, settlement, water level, and air pressure. All sensors connected to computer as recording system. The research object was soft soil prepared in the laboratory by simulating soil consistency conditions found in the field.

2.1. Testing Materials

Research materials for SAVP were obtained from disturbed and undisturbed soil samples collected around Gelora Bandung Lautan Api (GBLA) football stadium in Gedebage, Bandung, Indonesia. The parameters of the undisturbed soil sample at a depth of 2.5 m served as comparative data for SAVP results. Based on laboratory testing in soil mechanics, an undisturbed soil sample was found to be a silty clay with very soft soil parameters, as shown in Table 1.

Table 1. Parameters of undisturbed soil sample

Soil type	Soil weight units (kN/ m^3)		Consolidation parameters			
	γ_m	γ_d	C_c	C_v (m^2/sec)	m_v (m^2/kN)	e_0
Silty clay (MH)	13	5.58	0.93	0.0013	0.067	1.83

2.2. Testing Tools

GAVP was the result of collaboration among several engineering disciplines, including civil, geotechnical, electrical, and informatics, as shown in Figure 1. As a testing tool, GAVP was used to measure changes in soft soil parameters using sensors in the SAVP method, as shown in Table 1.

Figure 1. GAVP equipment in SAVP method test: (a) is soil sample tube, (b) is water circulation tank, (c) is reservoir for drained water from the PVD, (d) is vacuum pump, (e) is compressor, and (f) is monitor

Vacuum pump used was a submersible water pump, which functioned by converting kinetic energy into potential energy, pushing water from the ground to the surface. This pump had a submersible motor, which allowed complete submersion in the water tank for cooling while operating continuously for 24 hours. However, stopping the vacuum process directly affected the pore water pressure in soil.

2.3. Monitoring Position Scheme

In SAVP method, the spacing (s) between PVD was determined based on previous research. This showed that PVD had a cylindrical field of effect with an equivalent length [39]. The distance between PVD had to be less than the soft soil layer thickness [40]. The lateral permeability of the soil within the smear zone—disturbed by the use of a mandrel during PVD installation in the field—was found to range from 61% to 92% of the lateral permeability in undisturbed areas. Changes in soft soil parameters were monitored during the SAVP method testing, as shown in Figure 2-a, while the GAVP design model illustrates the field application of PVD installation [41, 42]. The tube dimensions, such as the base size of soil sample tube, were based on the diameter radius of vertical drainage (r_e) effect, considering the smear zone in Figure 2-b.

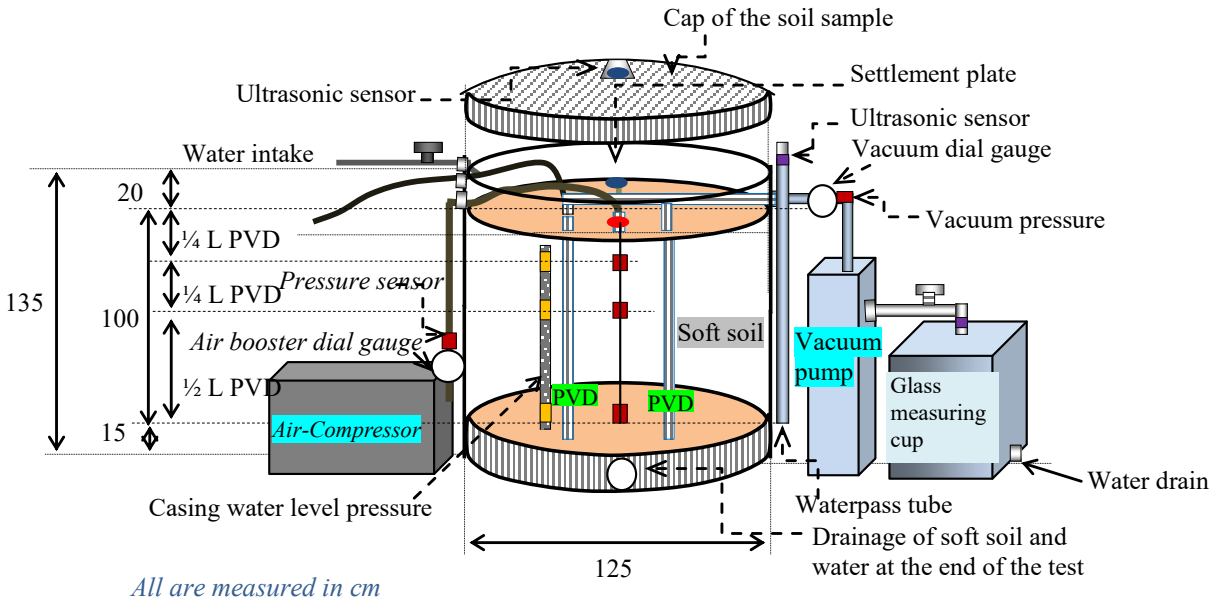

(a)

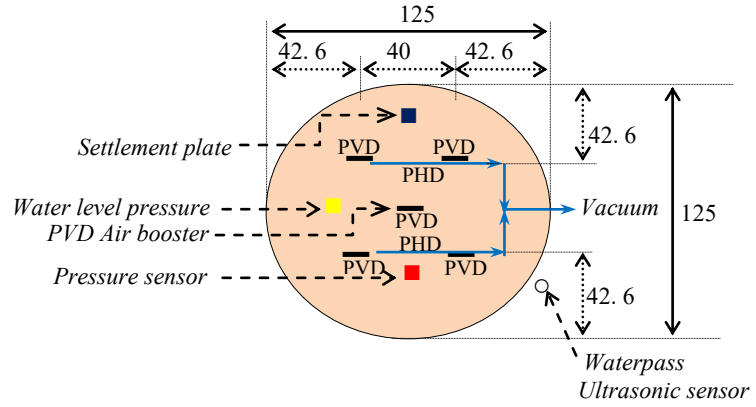

(b)

Explanation of the symbols in Figure 2: L PVD is length of PVD

1. Water level pressure, a sensor for pore water pressure
2. Ultrasonic sensor, a sensor for ground subsidence and groundwater level reduction
3. Water flow sensor, a sensor for drained water discharge from PVD
4. Pressure transducer sensor, a sensor for air booster pressure, vacuum, and preloading combination pressure sensors

Figure 2. Sketch of (a) GAVP apparatus and (b) top view of monitoring position

The research by Barron [43] showed that the smear zone was approximately 3-4 times. Based on this, the effective diameter of vertical drainage (d_e) was calculated to be 3-4 times larger than the hole caused by the mandrel (≈ PVD

width in the Laboratory). Using PVD width to be 10 cm, $d_e = 4 \times 10$ cm = 40 cm, and the distance between PVD or $s = d_e / 1.128 = 35.5$ cm. The distance between PVD was 30 cm, and the diagonal distance from the center between PVD was 21.2 cm [18].

The base size of GAVP soil sample tube was carefully selected to prevent disturbance of the smear zone, thereby preserving the lateral soil permeability, during the installation of PVD as a replacement for air pipe. The distance between PVD and s was taken as 40 cm, which was greater than 35.5 cm. The effective diameter was calculated as $d_e = 1.128s = 45.12$ cm, and the length of PVD was set at $2d_e = 90.24$ cm, which was approximately 90 cm but taken as 100 cm for SAVP method. The design size of SAVP method testing tool in laboratory used a distance between of 40 cm and a PVD length (L PVD) of 100 cm. Subsequently, pore water pressure measurements were carried out at three depths, namely ¼ L PVD (25 cm), ½ L PVD (50 cm), and L PVD (100 cm). The preloading combination pressure was monitored at soil surface, with depths of ¼L PVD (25 cm), ½L PVD (50 cm), and L PVD (100 cm). PVD length and equivalent diameter used in previous research included 100 cm and $d_e = 49.5$ cm [41], 110 cm and $d_e = 56$ cm [16], as well as 45 cm and $d_e = 33.8$ cm [18]. The distance between PVD in SAVP method was 40 cm, considering the smear zone to prevent disturbance by the monitoring instrument, as shown in Figure 3.

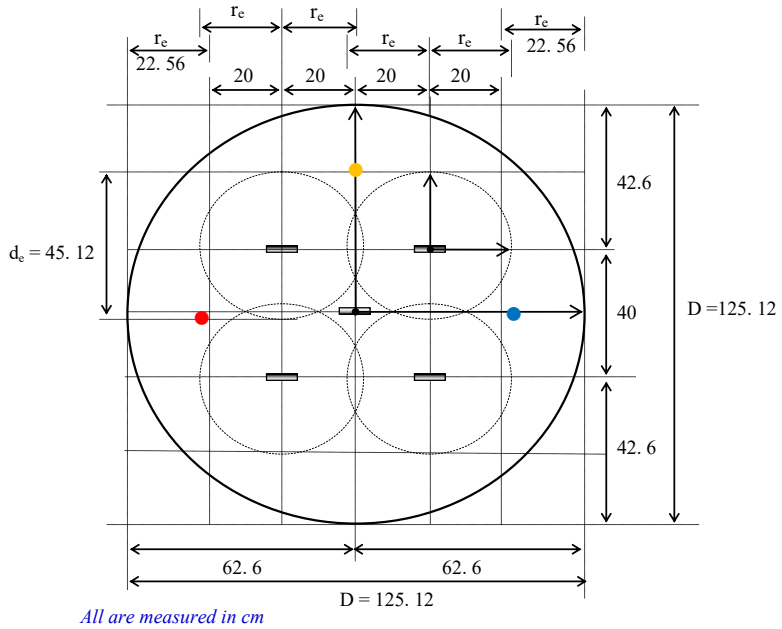

Figure 3. Base of SAVP method soil sample tube: ● : Pressure transducer, ● : Water level pressure, ● : Ultrasonic, ▬ : PVD

2.4. Testing Procedure

The SAVP method testing used GAVP that consisted of a soil sample tube with a diameter of 125 cm and a height of 135 cm. This tool was equipped with various sensors, including a soil sample settlement and a groundwater level subsidence monitoring system, both of which used ultrasonic sensors. Additionally, a monitor and a computer application program were used alongside a water circulation tank and a discharge monitoring system equipped with water flow sensors. A vacuum pump and an air compressor, both outfitted with pressure transducers, were also part of the experimental setup. The pore water pressure monitoring system included a water level pressure sensor, while the combined preloading used a pressure sensor. There was a wastewater reservoir and testing procedure simulated in-field soft soil improvement work, as shown in Figure 4-a. The water circulation tank acted as a storage unit for water from the vacuum pump and housing. Meanwhile, water from the tank served as both a coolant and a power source. The discharge system from the water circulation tank was integrated with a flow sensor to monitor the drained water discharge from PVD, as shown in Figure 4-b.

Figure 4. Monitoring exercise (a) water withdrawn from soil sample tube and (b) water discharge drained from the PVDs

PVD was attached to a steel frame anchor integrated into the tube base to maintain position changes during testing. A total of four drainage PVD, each 100 cm long and spaced 40 cm apart, were installed in a rectangular configuration. Meanwhile, one air pressure distribution PVD was placed in the center of the configuration.

Preloading combination pressure was monitored using pressure sensors placed at four depths, namely on the surface, 25 cm, 50 cm, and 100 cm. These sensors were able to monitor pressure ranging from -100 kPa to +100 kPa, as shown in Table 2. The ranging values were because preloading combination pressure was a combination of sucking vacuum (negative) and air pressure that was pushing (positive). Furthermore, pore water pressure was monitored using a water level pressure sensor placed at three depths, namely 25 cm, 50 cm, and 100 cm. Air booster pressure was monitored with a transmitter sensor, and vacuum preloading used a vacuum pressure transmitter sensor placed outside soil sample tube.

Table 2. Sensor specifications of the GAVP Tool

No.	Sensor specification					
	Parameter	**Sensing method**	**Sensor**	**Resolution**	**Range**	**Unit**
1	Discharge of water drained from PVD	Water flow	Water flow sensor	0.833	0.833 –16.6	ml/s
2	Soil settlement	Ultrasonic	Level sensor	0.1	0 – 140	cm
3	Groundwater level decline	Ultrasonic	Level sensor	0.1	0 – 140	cm
4	Pore water pressure	Water pressure	Water level pressure sensor	1	0 – 500	kPa
5	Air booster pressure, vacuum, and preloading combination pressure	Pressure transducer	Vacuum pressure transmitter	1	-100 – 100	kPa

A perforated casing pipe was installed inside soil sample tube, connected to external water level measuring pipe equipped with an ultrasonic sensor stored on the inside. For soil-level settlement monitoring, sensor was placed on the cover of the inner soil sample tube above the settlement plate. This sensor faced a thin settlement plate on soil surface. As the soil surface dropped, there was a corresponding decrease in monitored plate.

The testing material consisted of very soft soil sample from sub-chapter 2.1 that was made into soil slurry by soaking for 24 hours. This process was essential to prevent slurry from damaging internal instrument when poured into 1.5 m^3 tube. Subsequently, soil slurry was allowed to settle for 2 to 3 days, where excess water was removed through a perforated blanket pipe containing palm fiber as a filter. The blanket pipe had the same height as soil sample installed vertically in the tube and connected to a water drain pipe. This was followed by pouring of soil slurry, as shown in Figure 5. After filling below PHD installation and allowing settlement, the tube was tightly closed and prepared for testing.

Figure 5. Pouring soil slurry into soil sample tubes

The capacity of the field area that can be worked by one vacuum pump is 600 m^2, with PVD installation depth exceeding 20 m, based on the work experience of Teknindo Geosistem Unggul company. Before implementation, preliminary testing was required in the laboratory to obtain initial information that water from the 1.5 m^3 soil sample could be sucked out in less than 2 hours. Continuous testing beyond this point would cause the vacuum pump to overheat. Consequently, the testing duration was set, and the activation time of air pressure and vacuum preloading was adjusted based on the required capacity.

Air pressure and activation duration in SAVP method testing were based on the type of vacuum pump used and references from Lei et al. (2019) [18], Ke et al. (2019) [17], and Anda et al. (2020) [19]. An excessively long air booster activation duration caused a large amount of air to remain in soil, which led to small cracks, decreased vacuum [17], and high permeability [19]. Lei et al. (2019) [18] conducted AVP method testing using air pressure of 150 kPa and vacuum of 80 kPa, showing a significant gap in air booster pressure that should be determined before testing. However, vacuum preloading could not be established due to the type of pump, as the strength was generated by the pump's operation during testing. The specific preloading and duration of activating pressure in the SAVP method are shown in Table 3.

Table 3. The amount of pressure and activation monitored on the GAVP monitor

Preloading	Pressure (kPa)	Time (minutes)		
		50	10	49
Vacuum	-95	active	active	active
Air booster	+57	active	inactive	active

3. Theoretical Basis

The rectangular PVD installation configuration was based on the vertical drainage diameter (d_e) [42, 43]. The d_e value for the rectangular vertical drain configuration, as shown in Equation 1-a, was greater than triangular configuration in Equation 1-b. However, the distance between PVD for the rectangular configuration was smaller compared to the triangular configuration.

$$d_e = 1.128\ s \tag{1-a}$$

$$d_e = 1.050s \tag{1-b}$$

in which, s is distance between PVD and d_e is diameter of vertical drainage.

Vertical drains were based on radial consolidation theory [42, 44], where PVD settings, such as length and spacing, affected consolidation degree [45]. The equivalent drainage diameter of a ribbon-shaped PVD (d_w) [12] was defined as shown in Equation 2.

$$d_w = \frac{(b + t)}{2} \tag{2}$$

in which, b is PVD width and t is PVD thickness.

The water discharge drained from PVD was closely related to soil permeability. The decrease in water discharge or the slowing down of the water discharge drained from PVD was defined as shown in Equation 3.

$$a_q = \frac{q_1 - q_2}{t_2 - t_1} \tag{3}$$

in which, a_q is the deceleration of the drained water discharge from the PVD, q_1 is the drained water discharge from PVD at time t_1, and q_2 is the drained water discharge from the PVD at time t_2.

Soil permeability coefficient (k) = $f(T, S,\gamma_w, H,t,\sigma_{pc})$ was a function of time, soil surface settlement, unit weight of water, soil thickness, time, and combined preloading pressure. The vertical permeability of soil (k_v) under these conditions was equal to the horizontal permeability (k_h), or $k_v = k_h$. Specifically, soil permeability coefficient can be defined as shown in Equation 4.

$$k_v = \frac{TS\gamma_w H}{t\,\sigma_{pc}} \tag{4}$$

in which, k is vertical permeability coefficient, T is time factor, σ_{pc} is combined preloading pressure, γ_w is unit weight of water, S is soil surface settlement, H is soil thickness, and t is time.

Generally, time factor (T) affects soil permeability coefficient. This parameter serves as a function of the volume of water drained from PVD, the combined preloading pressure, the unit weight of water, the soil surface settlement, and the total volume of water. The time factor can be expressed as a mathematical function, namely, $T = f(V_i, \sigma_{pc}, \gamma_w, S, \Sigma V_i)$, which is defined as shown in Equation 5.

$$T = \frac{V_i\,\sigma_{pc}}{\gamma_w\,S\,\Sigma V_i} \tag{5}$$

in which, T is time factor, V_i is water volume at time i, σ_{pc} is combined preloading pressure, γ_w is unit weight of water, S is soil surface settlement, and ΣV_i is total water volume at time i.

Consolidation coefficient, mathematically expressed as $C_{vr} = f(k, H,\sigma_{pc}, S,\gamma_w)$, was a function of soil permeability, soil thickness, combined preloading pressure, soil surface settlement, and unit weight of water. This parameter is defined as shown in Equation 6.

$$C_{vr} = \frac{k_v H\sigma_{pc}}{S\gamma_w} \tag{6}$$

in which, C_{vr} is radial soil consolidation coefficient, σ_{cp} is combined preloading pressure, γ_w is unit weight of water, S is soil surface settlement, k_v is vertical soil permeability coefficient, and H is soil thickness.

Soil volume compression coefficient was a function of soil surface settlement, soil thickness, and combined preloading pressure. Expressed as $m_v = f(S, H, \sigma_{pc})$, soil volume compression coefficient was defined as shown in Equation 7-a. Meanwhile, soil settlement was the product of soil volume compression coefficient, thickness, and combined preloading pressure, or $S_i = f(m_{vi}, H_i, \sigma_{cpi}(t))$, defined as shown in Equation 7-b.

$$m_v = \frac{S}{H\,\sigma_{pc}} \tag{7-a}$$

$$S = m_v\,H\,\sigma_{pc} \tag{7-b}$$

in which, m_v is soil volume compression coefficient, σ_{pc} is preloading combination pressure, S is soil surface settlement, and H is soil thickness.

The total soil settlement was calculated by combining the subsidence during PVD installation [5]. Meanwhile, final land subsidence (S_f) was determined using the method by Chu et al. [5], defined as shown in Equation 8.

$$S_f = \frac{S_3(S_2 - S_1) - S_2(S_3 - S_2)}{(S_2 - S_1) - (S_3 - S_2)} \tag{8}$$

in which, S_1 is soil surface settlement at time t_1, S_2 is soil surface settlement at time t_2, dan S_3 is soil surface settlement at time t_3.

Soil surface settlement was measured at time t, which continued to increase until the end of the testing at time t_3. Consolidation (U) is the ratio of soil surface settlement at time t (S_t) to the final soil surface settlement [3], defined as shown in Equation 9.

$$U = \frac{S_t}{S_f} \tag{9}$$

in which, U is consolidation degree

4. Results

The 109-minute testing showed an average air pressure of +57 kPa (positive) when activated. However, air pressure did not return to zero kPa when deactivated, and a vacuum preloading of -95 kPa (negative) was recorded on the monitor, as presented in Figures 6-a and 6-b, respectively. Air holes on the surface of the soil sample were found when the test was completed as can be seen in Figure 7. These air holes became a medium for the flow of air pressure from the bottom of the soil sample to the surface due to the air pressure coming out of the tip of the PVD, even though the air pressure given was relatively small compared to previous researchers.

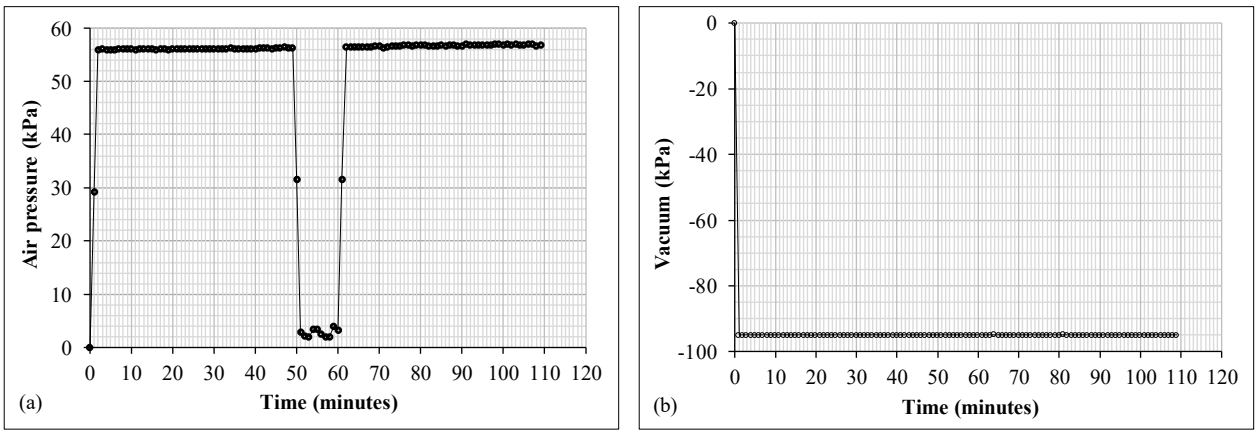

Figure 6. Preloading of (a) air booster pressure (b) vacuums

Figure 7. Physical changes to the soil surface

The combined preloading pressures from four depths, the average combined pressure on the soil sample, the effect of air pressure and vacuum, and the effect of air pressure and time as can be seen in Figures 8-a to 8-d, respectively.

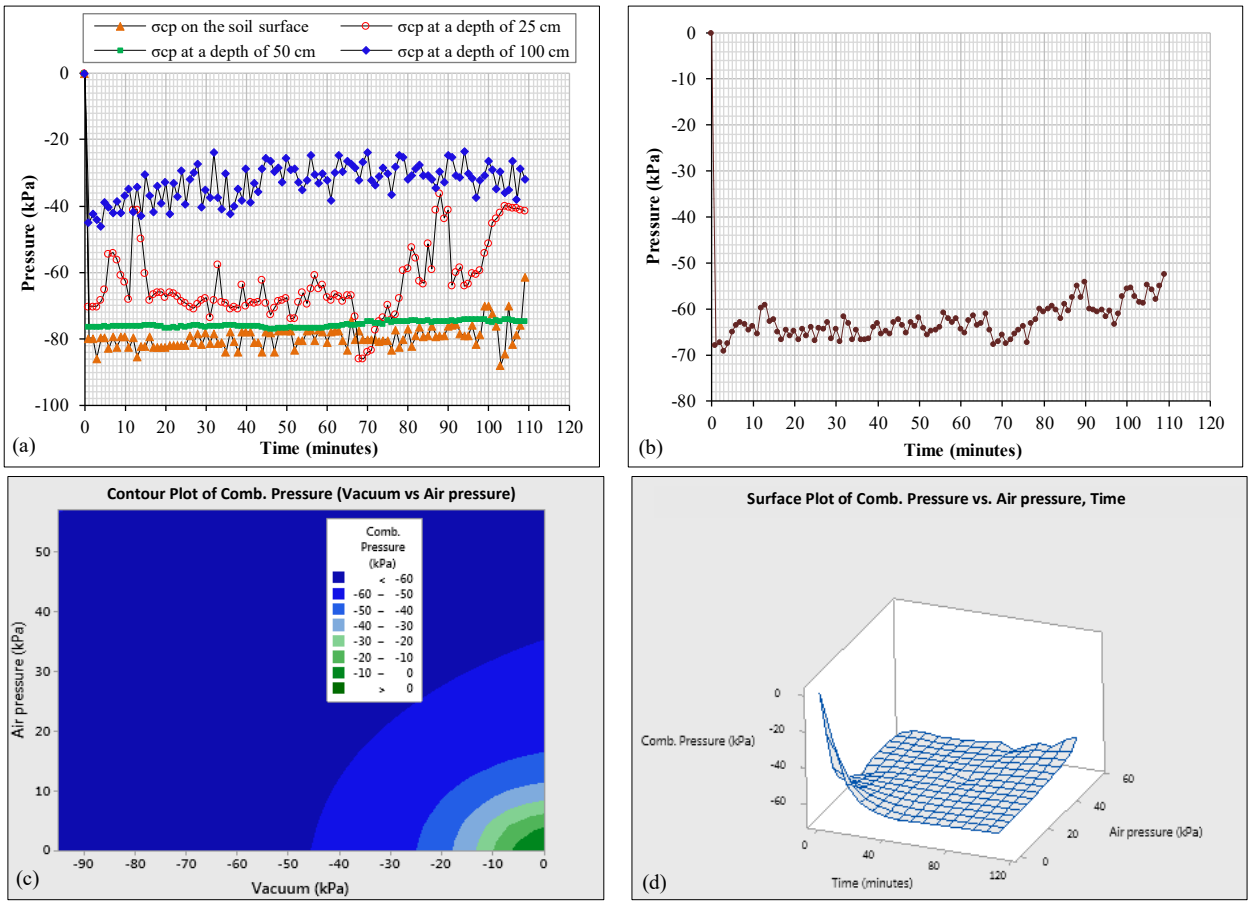

Figure 8. Combined preloading pressures (a) four soil sample depths, (b) average of soil samples, (c) vacuum and air pressure effect, and (d) air pressure and time effect

The average preloading combination pressure on the surface of the soil sample was recorded at -79.41 kPa (negative). The average preloading combination pressure at a depth of 25 cm is -63.04 kPa (negative), which depicts a fluctuating graph; this is the effect of air trapped on the surface of the soil sample. At a depth of 50 cm, the average preloading combination pressure was -75.60 kPa (negative), showing a stable condition graph due to the balance of vacuum and air pressure. However, at a depth of 100 cm, a value of -32.77 kPa (negative) was obtained, indicating very strong pressure at the air outlet zone. The average preloading combination pressure on the soil sample was -62.7 kPa (negative) overall over time, tending to increase towards the air pressure influence zone; this indicates that the air pressure on the soil sample remains due to the large and long activation of the air pressure even though the vacuum pump remains active.

4.1. Drained Water Flow from PVD

The increase in drained water flow from PVD showed permeability of soil, which was affected by the presence of air channels connecting the bottom of the soil sample to the surface, resulting from air pressure. Changes in drained water flow from PVD from the 13th to the 24th minute showed fluctuating water flow, while monitoring of vacuum and air booster pressure indicated a constant condition. Furthermore, the total volume of water drained from PVD during the 109-minute testing was 719.3 liters. The fluctuating water flow was caused by the placement of the water flow sensor on the outlet pipe from the circulation tank. The drained water flow from PVD stabilized from the 25th minute until the end of the testing. This was because water stored in the circulation tank was sufficient to pass back through the flow sensor, although there was a slight decrease in some areas. There was a slight decrease in drained water flow from the 50th to the 60th minute when the air compressor was inactive.

The drained water discharge from PVD and the decrease in groundwater level are shown in Figures 9-a and 9-b, respectively. The final decrease in groundwater level was 13.04 cm during the testing. Statistical tests using Minitab 19 software on the regression equation of groundwater level decline (GWL) against water discharge (q) and time (t) obtained: GWL = -0.06804 - 0.3391q (liters/sec) - 0.000419t (minutes), p-value for water discharge of 0.000 and p-value for time of 0.003, p-value < 0.05 means that water discharge and time are very significant to groundwater level decline; The regression equation of air pressure, vacuum, and time against water discharge obtained: q (liters/sec) = 0.0001 - 0.000774vacuum (kPa) - 0.000481air pressure (kPa) + 0.001105t (minutes). The P-Value of vacuum, air pressure, and

time are 0.018, 0.007, and 0.000, respectively. P-value < 0.05 means that the influence of vacuum, air pressure, and time is very significant on water discharge. The effect of preloading on water discharge can be seen in Figure 9-c. The relationship between permeability and time on water discharge can be seen in Figure 9-d.

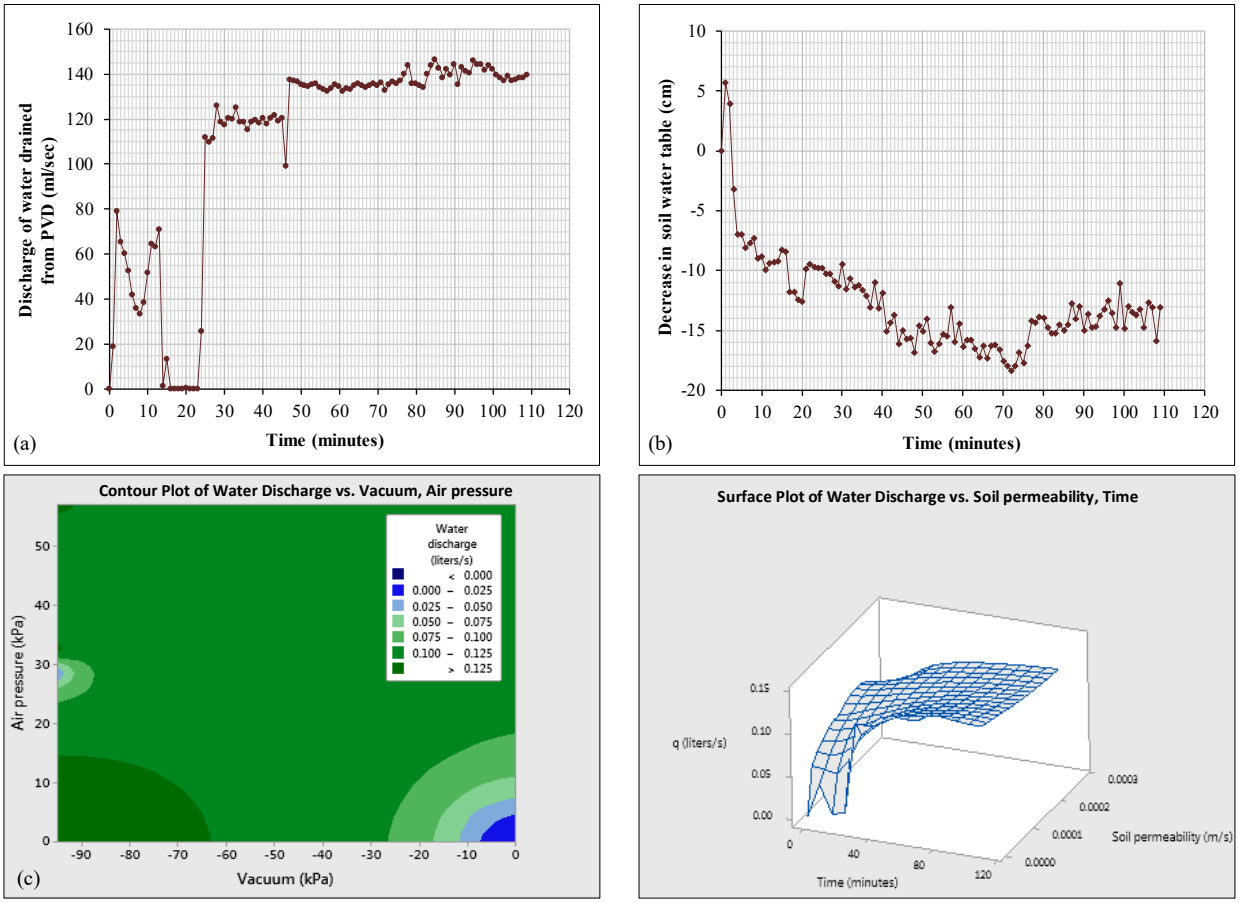

Figure 9. Changes in (a) discharge of water drained from the PVD, (b) decrease in groundwater level, (c) water discharge due to vacuum and air pressure, and (d) water discharge due to the influence of permeability

Changes in discharge affected the decrease in groundwater level and increase in pore water pressure during the time interval from the 50th to the 60th minute, as shown in Figure 10-a. The pore water pressure at preloading equilibrium of 4.29 kPa is at a depth of 50 cm (in the middle of the soil sample depth). The average pore water pressure of the soil sample is 2.17 kPa as a result of the GAVP tool. The statistical results of Minitab 19 software from the relationship between vacuum and air pressure to the average pore water pressure of the soil sample can be seen in Figure 10-b.

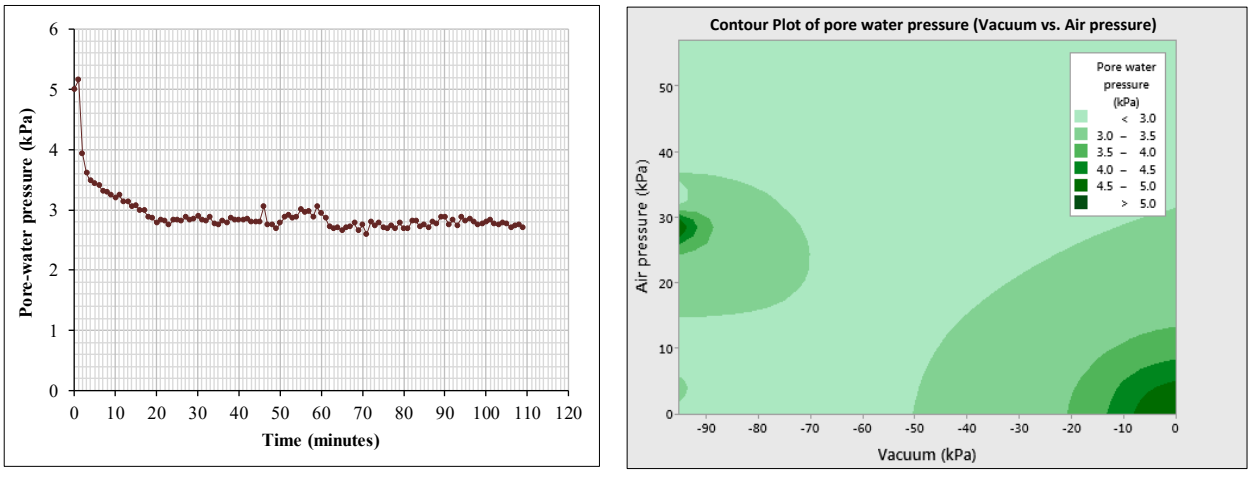

Figure 10. Changes in average pore water pressure of (a) soil and (b) the effects of vacuum and air pressure

The results obtained an average air pressure when actively monitored at +57 kPa (positive) and not truly zero kPa when not activated. This was because air pressure remained in soil sample from the previous air pressure application. The average pore water pressure of the soil sample, from the 50th to 60th minute, showed an increase due to the inactivity of air compressor. However, pressurized air remained in sample from the previous air pressure, which was indicated by a decrease in water level and the combined preloading pressure, showing the effect of air pressure.

During the testing, the drained water discharge from PVD at the 55th minute (q_1) was measured at 134.33 ml/sec, while at the 109th minute (q_2) it was 139.60 ml/sec. Consequently, the slowdown in water discharge from PVD (a_q) was recorded at 0.001 ml/sec² or 4.06 ml/min². The drained water discharge had slowed down over time due to the reduction in water content and air trapped in soil sample. A significant issue occurred between the 13th and 24th minute, in line with air booster pressure and vacuum preloading, causing water in the circulation tank to be pushed. Therefore, water level was slightly reduced, making it difficult for flow sensor to monitor discharge accurately (This situation also led to abnormal changes in soil parameters).

4.2. Soft Soil Parameters

Soft soil showed poor characteristics, including low bearing capacity, significant deformation, reduced consistency, decreased permeability, a very low consolidation coefficient, a high volumetric compression coefficient, and a tendency to deform easily under load. Therefore, this research examined the combined effects of preloading pressure, drained water discharge from PVD, soil settlement, groundwater table, and changes in soft soil parameters such as permeability coefficient (k), consolidation coefficient (C_c), and volumetric compression coefficient (m_v), as well as the relationships between these parameters.

4.2.1. Soil Permeability Coefficient

Soft soil parameter data included permeability coefficient, consolidation coefficient, and volumetric compression coefficient. Since soft soil parameters were very small, the values were multiplied by 10^7 or E+07 using a logarithmic scale to visualize the graph. The units were also multiplied by 10^{-7} or E-07 as shown in Figures 11 to 15. The average soil parameter values, recorded at 10-minute intervals, are presented in Table 4.

Table 4. Soft soil parameters of SAVP method test results per five minutes of testing

Time (min)	Soil permeability coefficient (mm/sec)	Consolidation coefficient (m²/sec)	Soil volume compression coefficient (m²/sec)
0	0.00	0.00	0.00
10	3.00E-03	8.63E-05	2.75E-03
20	1.07E-05	2.96E-07	2.66E-03
30	7.68E-04	2.08E-05	2.78E-03
40	3.21E-04	7.17E-06	3.11E-03
50	1.95E-04	4.03E-06	3.34E-03
60	1.20E-04	2.86E-06	3.07E-03
70	8.17E-05	1.63E-06	3.16E-03
80	5.96E-05	1.29E-06	3.56E-03
90	4.79E-05	8.71E-07	4.70E-03
100	3.68E-05	6.83E-07	4.20E-03
109	2.97E-05	5.87E-07	4.70E-03

The average soil parameter values recorded during testing for soil permeability coefficient, consolidation, and volumetric compression were 4.60E-03 mm/s, 1.93E-04 m²/s, and 3.26E-03 m²/kN, respectively. Permeability coefficient observed at each depth was related to the distance from the examined position to air pressure source outlet, combined preloading pressure, water discharge from PVD, time, and the performance of vacuum pump, as shown in Figure 11.

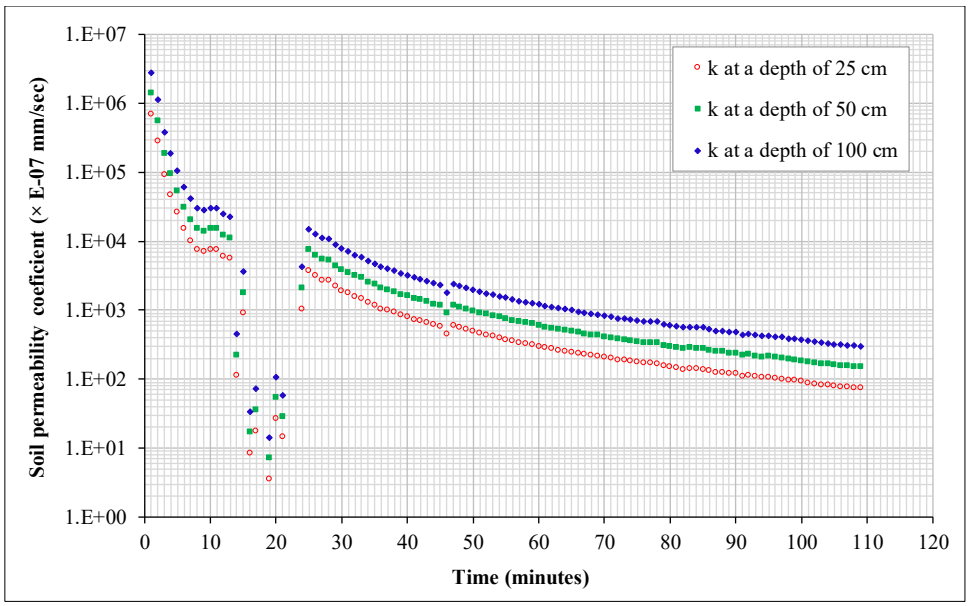

Figure 11. Permeability coefficients of soil samples from three monitoring depths

Permeability coefficient of soil sample remained constant in the testing at 0.0046 mm/s, with an average value of 3.2E-05 mm/s. Table 5 shows the average permeability coefficient in the testing from the 100th to the 109th minute.

Table 5. Average permeability coefficient of the soil sample

Depth Soil sample (m)	Soil permeability coefficient (mm/sec)	
	During the test	At the end of testing
25 cm	1.2E-03	8.0E-06
50 cm	2.3E-03	1.6E-05
100 cm	4.6E-03	3.2E-05
Average of the soil samples	4.6E-03	3.2E-05

4.2.2. Consolidation Parameters

In this research, radial consolidation coefficient (C_{vr}) was the same as consolidation coefficient (C_v) because vacuum effectively drew groundwater through PVD. Observation showed that consolidation coefficient at the three depths decreased over time, as shown in Figure 12. This corresponded to a decrease in the combined preloading pressure of soil samples, as further shown by soil volume compression coefficients at the three depths in Figure 13.

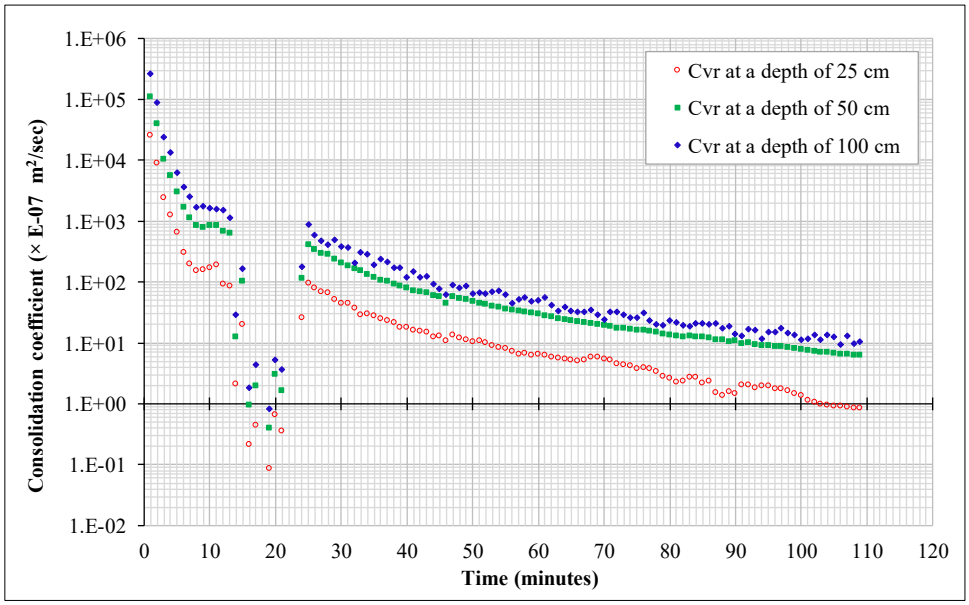

Figure 12. Consolidation coefficients of three depths of soil samples

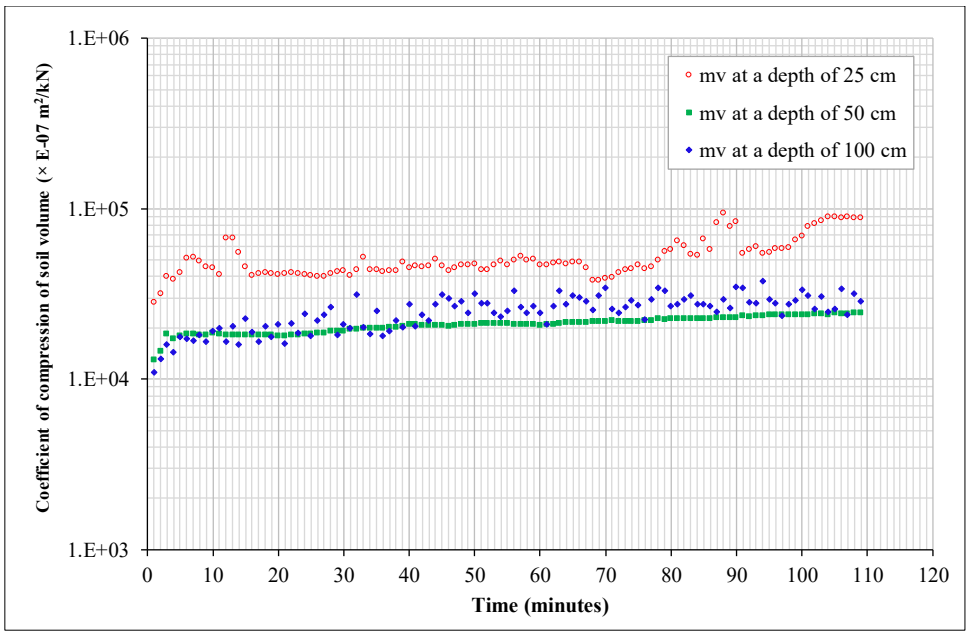

Figure 13. Volume compression coefficient of soil samples from three monitoring depths

The coefficients of consolidation and compression of the natural soil volume of soil sample were 0.0013 m²/sec and 0.067 m²/kN, respectively, as shown in Table 1. During the first five minutes of preloading, coefficient of consolidation and compression of soil volume were 0.012 m²/s and 0.00092 m²/kN, respectively. At the end of the test, these values were reflected in Tables 6 and 7.

Table 6. Average consolidation coefficient of soil sample

Depth soil sample (m)	Consolidation coefficients (m²/sec)	
	During the test	At the end of testing
25 cm	4.0E-05	9.5E-08
50 cm	1.7E-04	6.8E-07
100 cm	3.8E-04	1.2E-06
Average of the soil samples	5.8E-04	2.0E-06

Table 7. Average soil volume compression coefficient of soil sample

Depth Soil sample (m)	Coefficient of compression of soil volume (m²/kN)	
	During the test	At the end of testing
25 cm	5.2E-03	8.6E-03
50 cm	2.1E-03	2.4E-03
100 cm	2.5E-03	2.8E-03
Average of the soil samples	1.3E-03	1.6E-03

Consolidation coefficient at a depth of 25 cm was smaller due to the effect of strong air booster pressure and vacuum. At a depth of 50 cm, the value became more stable because of a balanced preloading combination pressure. Consolidation coefficient at air pressure outlet zone is compared to others due to the large air pressure. At the end of the testing, consolidation coefficient was 2.0E-06 m²/second, in line with the decreasing value of soil permeability coefficient. Soil volume compression coefficient at a depth of 25 cm fluctuated and was greater compared to values at 50 cm and 100 cm. At a depth of 50 cm, stability was observed due to the combination of preloading and pressure. Soil volume compression coefficient at a depth of 100 cm was small and fluctuated because of the high air pressure.

4.3. Relationship Between Soil Parameters

Figure 14-a shows the relationship between soil permeability coefficient and consolidation coefficient. Meanwhile, the relationship between consolidation coefficient and soil volume compression coefficient is presented in Figure 14-b.

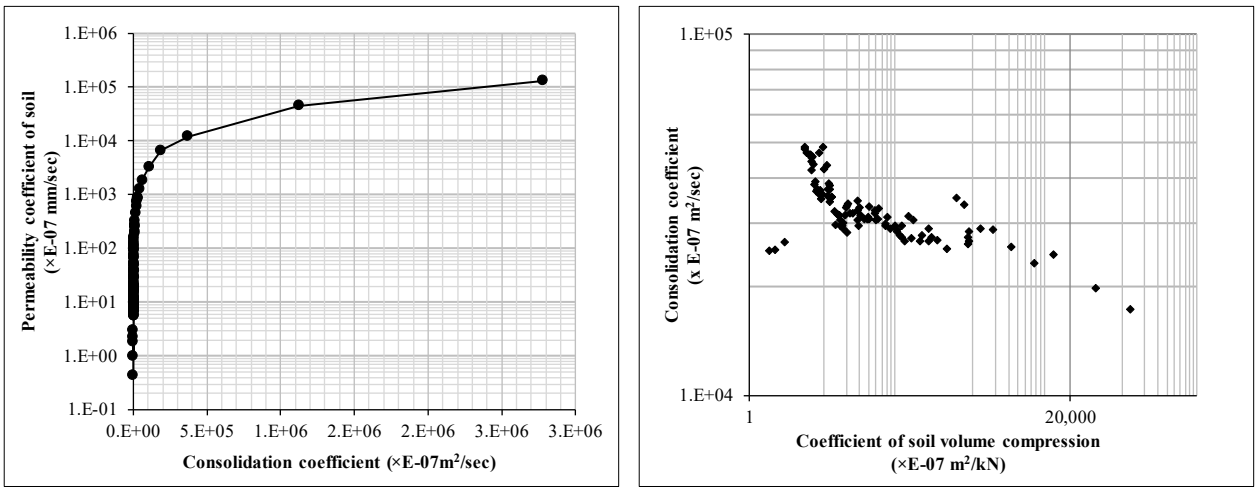

(a) (b)

Figure 14. Relationship of coefficient of (a) soil permeability to consolidation and (b) consolidation to soil volume compression

4.4. Abnormalities in Testing Results

Changes in soil parameters, as observed in the testing results, were shown in three parts of the time series of soil sample parameters due to drained water discharge from PVD. The first time change occurred from the start until the 12th minute. The second time change spanned from the 13th minute to the 24th minute, and the third was from the 25th minute until the end of the testing, as shown in Table 8. The pattern of changes in soil parameters from the 13th minute to the 24th minute was shown in Figures 15-a and 15-b for soil permeability and consolidation coefficient, respectively.

Table 8. Average soil parameters from three changeover times

Time (min)	Soil permeability coefficient (mm/sec)	Consolidation coefficient (m²/sec)	Consolidation coefficient (m²/sec)
0 – 12	4.01E-02	1.71E-03	2.60E-03
13 – 24	2.57E-04	6.96E-06	2.75E-03
25 – 109	2.12E-04	5.34E-06	3.43E-03

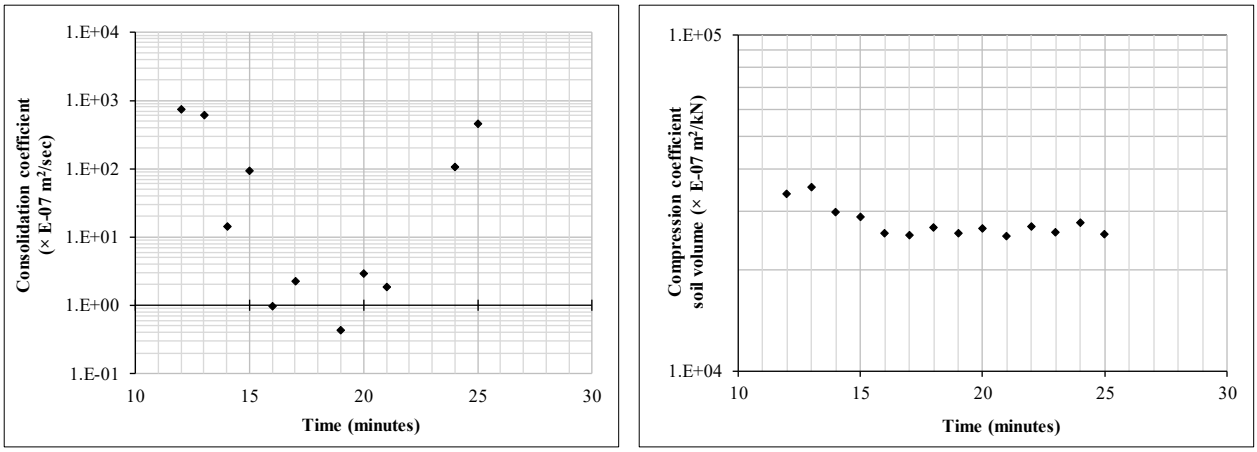

(a) (b)

Figure 15. Pattern of change in coefficients of (a) consolidation and (b) soil volume compression

During the crucial 13th to 24th minute of the soil parameter testing, both permeability and consolidation coefficient showed minimal change. However, soil volume compression coefficient remained unexpectedly low. This was unusual as volume compression was supposed to show a larger value or inversely proportional to consolidation coefficient. The abnormality was attributed to unstable drained water discharge from PVD, a situation predicted based on the sensor's placement on water discharge pipe from the circulation tank. At the beginning of the testing, water level in the tank decreased as it was strongly pushed by vacuum pump, which initially supplied water to refill the circulation tank. Therefore, water flow sensor was unable to read discharge until it started flowing back out of the discharge pipe from the tank. Since one of the factors affecting soil parameters was water discharge drained from PVD, the sensor's improper readings significantly affected the results of soil parameter research.

4.5. Relationship between Soil Volume Compression, Soil Settlement, and Consolidation

Soil settlement showed continuity in the same soil type, despite the different depths examined, as presented in Table 9. For instance, the magnitude of soil settlement at three depths at the 109th minute was calculated using Equation 7-b as follows: Depth (H) = 25 cm, combined preloading pressure (σ_{cp}) = -41.47 kPa, soil volume compression coefficient (m_v) 0.00881 m²/kN, therefore S = 9.14 cm; H = 50 cm, σ_{cp} = -74.73 kPa, m_v = 0.00245 m²/kN, S = 0.09137 m ≈ 9.14 cm; H = 100 cm, σ_{cp} = -32 kPa, m_v= 0.00286 m²/kN, S = 0.09137 m ≈ 9.14 cm. The final surface settlement of soil (S_f) was calculated using Equation 8, based on the monitoring data, showing S_1 = 7.02 cm at the 25th minute, S_2 = 8.08 cm at the 55th minute, and S_3 = 8.45 cm at the 85th minute. The calculation results obtained an S_f of 8.64 cm, while the monitoring values were 9.14 cm.

Table 9. Soil settlement monitored from several depths

Time (min)	Pre-loading combination pressure (kPa) at depth (cm)			Soil volume compression coefficient (m²/kN)			Soil settlement (cm)
	25	50	100	25	50	100	
0	0.00	0.00	0.00	0.00	0.00	0,00	0.00
10	-62.70	-76.03	-36.65	4.48E-03	1.85E-03	1.92E-03	7.03
20	-67.37	-76.70	-32.87	4.10E-03	1.80E-03	2.10E-03	6.90
30	-67.67	-76.40	-34.95	4.33E-03	1.92E-03	2.09E-03	7.32
40	-70.07	-76.00	-28.62	4.51E-03	2.08E-03	2.76E-03	7.89
50	-67.57	-76.73	-25.40	4.76E-03	2.09E-03	3.16E-03	8.04
60	-67.53	-76.37	-32.18	4.68E-03	2.07E-03	2.45E-03	7.90
70	-83.97	-74.73	-23.75	3.88E-03	2.18E-03	3.43E-03	8.14
80	-58.80	-74.53	-31.73	5.75E-03	2.27E-03	2.66E-03	8.45
90	-41.17	-74.77	-24.65	8.33E-03	2.29E-03	3.48E-03	8.57
100	-51.17	-74.57	-26.40	6.89E-03	2.36E-03	3.34E-03	8.82
109	-41.47	-74.73	-32.00	8.81E-03	2.45E-03	2.86E-03	9.14

The final soil settlement (S_f) and consolidation degree (U) based on the applied preloading were calculated using Equations 8 and 9, respectively. The values obtained were σ_{50}, S_f = 9.14 cm, U = 57.1%; σ_{50} + 10 kPa air pressure, S_f = 7.91 cm, U = 57.6%; σ_{50} + 20 kPa air pressure, S_f = 6.69 cm, U = 58.3%; σ_{50} + 10 kPa vacuum, S_f = 10.36 cm, U = 56.6%; σ_{50} + 20 kPa vacuum, S_f = 11.58 cm, U = 56.3%. Consolidation degree under several preloading conditions was determined by dividing soil settlement at time t by the final soil settlement under condition σ_{50}. The final soil settlement and consolidation degree for several preloading conditions are presented in Table 10 and Figure 16-a. The relationship between vacuum and air pressure on soil settlement can be seen in Figure 16-b.

Table 10. Soil settlement under different conditions from the effect of air pressure and vacuum

Time (minutes)	Combined preloading pressure (kPa)					m_{v50} (m²/kN)	Settlement of soil surface (cm)				
	σ_{50}	σ_{50} + 10	σ_{50} + 20	σ_{50} -10	σ_{50} -20		S_{50}	$S(\sigma_{50}+10)$	$S(\sigma_{50}+20)$	$S(\sigma_{50}$ -10)	$S(\sigma_{50}$ -20)
0	0.0	0.0	0.0	0.0	0.0	0.0	0.0	0.0	0.0	0.0	0.0
10	-76.0	-66.0	-56.0	-86.0	-96.0	1.9E-03	-7.0	-6.1	-5.2	-8.0	-8.9
20	-76.7	-66.7	-56.7	-86.7	-96.7	1.8E-03	-6.9	-6.0	-5.1	-7.8	-8.7
30	-76.4	-66.4	-56.4	-86.4	-96.4	1.9E-03	-7.3	-6.4	-5.4	-8.3	-9.2
40	-76.0	-66.0	-56.0	-86.0	-96.0	2.1E-03	-7.9	-6.9	-5.8	-8.9	-10.0
50	-76.7	-66.7	-56.7	-86.7	-96.7	2.1E-03	-8.0	-7.0	-5.9	-9.1	-10.1
60	-76.4	-66.4	-56.4	-86.4	-96.4	2.1E-03	-7.9	-6.9	-5.8	-8.9	-10.0
70	-74.7	-64.7	-54.7	-84.7	-94.7	2.2E-03	-8.1	-7.1	-6.0	-9.2	-10.3
80	-74.5	-64.5	-54.5	-84.5	-94.5	2.3E-03	-8.5	-7,32	-6,18	-9.6	-10.7
80	-74.5	-64.5	-54.5	-84.5	-94.5	2.3E-03	-8.5	-7,32	-6,18	-9.6	-10.7
90	-74.8	-64.8	-54.8	-84.8	-94.8	2.3E-03	-8.6	-7.4	-6.3	-9.7	-10.9
100	-74.6	-64.6	-54.6	-84.6	-94.6	2.4E-03	-8.8	-7.6	-6.5	-10.0	-11.2
109	-74.7	-64.7	-54.7	-84.7	-94.7	2.5E-03	-9.1	-7.9	-6.7	-10.4	-11.6
Degree of consolidation (U, %)							**57.1**	**49.6**	**42.1**	**64.5**	**72.0**

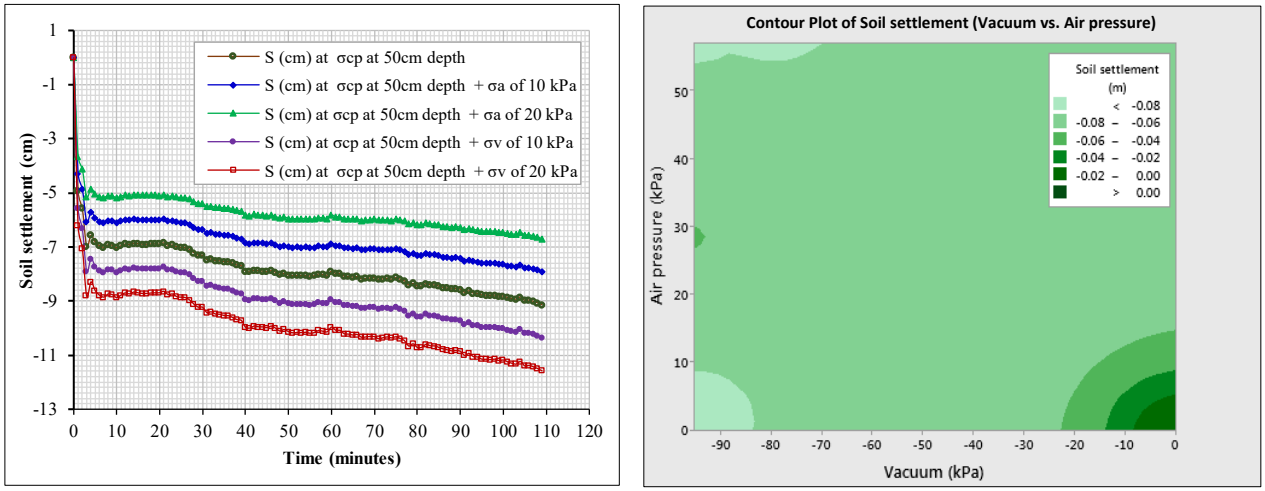

(a) (b)

Figure 16. Soil surface settlement at (a) multiple preloading and (b) the effects of vacuum and air pressure

5. Discussion

The laboratory SAVP method uses GAVP for testing soil samples from the field to obtain vacuum size and air booster pressure. In this method, PVD is used as drainage and conduit for channeling air booster pressure into soil. A major advantage is the use of air-conducting PVD without removal after construction, thereby preventing buckling in PVD that can affect the behavior of soft soil. Furthermore, SAVP method has been proven effective as a solution to blockages in PVD drainage. The long-term performance and durability of this method are possible, particularly when air-conducting PVD can be produced at the factory level. GAVP becomes a measuring tool for soil settlement and groundwater level decline in real time. Regardless, changes are needed, specifically in the instruments' installation and in the sensors' placement. The success of SAVP method depends significantly on the ability to reliably extrapolate experimental results to real-world scenarios.

PVD drainage functions as a permeable medium, facilitating water removal from soft soil during consolidation [46]. In numerical modeling, PVD drainage and the improved soil are commonly treated as identical in a plane strain framework [47]. The effectiveness of PVD drainage is directly linked to increases in soil shear strength [48]. However, its drainage capacity can be compromised by clogging, which occurs when very fine soil particles infiltrate PVD core during consolidation [7, 49]. To address this issue, SAVP method has been proposed, which gradually applies air pressure to temporarily block drainage without diminishing vacuum strength.

Experimental observations show that the average permeability coefficient of soil samples at a depth of 100 cm is higher than 25 cm and 50 cm. This suggests increased permeability in air outlet zone, likely due to elevated air pressure and the influence of drainage openings located at the bottom end of air-conducting PVD. During the initial five minutes of preloading, the average soil permeability coefficient reached 0.091 mm/s, while silty clay shows permeability coefficients in the range of 10^{-3} mm/s. These results indicate that air pressure substantially enhances soft soil permeability, as well as consolidation and volume compression coefficients.

In this research, permeability coefficients at all three monitored depths were influenced by the volume of water discharged through PVD. After testing period, permeability coefficient significantly decreased due to reduced water content and the presence of residual air in soil matrix. As water content diminishes, soil volume compression coefficient tends to increase. This suggested a gradual reduction in soil compressibility, caused by rising air pressure and declining vacuum pump efficiency due to air accumulation in the sample. Since consolidation coefficient is a function of soil permeability, it shows a direct proportionality to permeability coefficient. The graphical representation of this relationship is often in a parabolic form, which is attributed to differential soil settlement during consolidation process.

Soil settlement is the product of soil volume compression coefficient, thickness, and combined preloading pressure, which serves as a function of time. In this research, soil settlement was analyzed using soil volume compression coefficient at a thickness of 50 cm, combined preloading pressure at a depth of 50 cm (σ_{50}) as the independent variable. The results in Table 10 showed that air pressure was reduced by 20 kPa to produce optimal settlement of 11.58 cm and consolidation degree of 72.0%. However, when air pressure increased by 20 kPa, the soil settlement was 6.69 cm and consolidation degree was 42.1%. This indicated that air pressure affected soil settlement and consolidation degree.

The SAVP method is basically an effort to remove water from the pore space in water-saturated soil which can be applied to soil with different clay minerals or organic content, this is because this method is physical in nature in the form of energy distribution from vacuum preloading and measured air pressure. The sensors used in the GAVP tool

before the experiment were calibrated according to their function, for example, the pore water pressure sensor was initially checked on static pore water pressure, the ultrasonic sensor was based on distance, the pressure sensor for vacuum and air pressure from the compressor was compared to a manometer or non-digital dial to ensure measurement accuracy, while the results of the experiment were compared with the results of standard tools commonly used in soil laboratories. The distance between PVDs in laboratory research is set at 40 cm (considering the smear zone) according to the literature review in sub-chapter 2.3. If the distance between PVDs is smaller for deeper layers, the results will be according to the PVD installation configuration and the diameter of the vertical drainage influence (d_e).

Wang et al. [15] reported that applying vacuum and air pressure accelerates the improvement of soft soils. However, the influence of air-pressure magnitude had not been examined in the study by Lei et al. [18]. Ke et al. [17] investigated the effect of air-pressure duration and showed that the length of air-pressure application influences both pore-water pressure and vacuum levels. Accordingly, the SAVP method regulates air pressure and application time to achieve a balanced preloading pressure combination, as illustrated in Figure 8(a), thereby enhancing the degree of consolidation. Permeability affects consolidation, where in the air pressure outlet zone, namely at a depth of 100 cm, the permeability increases, so that it can cause uneven consolidation, so a special factory-made air distribution PVD is needed to be able to distribute the same amount of air pressure at several depths to avoid uneven consolidation.

The abnormality observed between the 13th and 24th minutes is caused by the position of the water-discharge sensor, which is located on the circulation-tank pipe and is not directly passed by water. This issue would not occur if the sensor were installed in a location unaffected by the water pressure generated by the vacuum pump, even though field conditions often involve unstable water flow and fluctuating groundwater levels. Adjusting the air-pressure input can control excessive vacuum loss caused by the formation of air channels by balancing the combined preload pressure. If only vacuum is applied (vacuum loading method), previous studies have shown that clogging may occur in the PVD filter. Therefore, laboratory testing is essential before field implementation to ensure optimal performance, as each soil type has distinct characteristics. The SAVP method is a modified version of the AVP technique and differs from the gradual air-pressure approach. Its effectiveness lies in the use of sensors capable of monitoring real-time changes in soil parameters at multiple depths. In contrast, the SVP method, when applied with gradual vacuum adjustment, can help reduce the risk of PVD filter clogging [13].

6. Conclusions

In conclusion, this research shows that soil parameters and the correlation between soil properties can be comprehensively examined. The results obtained are as follows:

- High air pressure and prolonged active time affect soil permeability and the drained water discharge from PVD; Air pressure causes an increase in the drained water discharge from PVD, which includes changes in soft soil parameters, and air pressure can increase soil permeability.
- Consolidation coefficient is small due to the same air pressure and vacuum strength; Furthermore, soil permeability and consolidation coefficients decrease at the end of the testing because of long active time of air pressure; Consolidation coefficient is high due to air pressure performance, although it does not affect consolidation; and The large soil volume compression coefficient is due to the same air pressure and vacuum strength.
- The parabolic graph pattern of the relationship between consolidation and soil permeability is caused by the soil settlement that occurs; Consolidation coefficient is inversely proportional to soil volume compression coefficient; However, variations in the results occur when the drained water discharge from PVD presented by the monitor is unstable.
- The balance of preloading combination pressure affects soil volume compression, soil settlement, and consolidation. Based on the relationship analysis, soil settlement is continuous for the same soil type and is a function of time. The results also show that air pressure affects soil settlement and consolidation degree.

Based on the analysis, further research is required to improve very soft soil using the combined pressure method, integrating both air pressure and vacuum in SAVP, to obtain a standard formula for preloading combination pressure balance.

6.1. Derivation of Soil Parameter Equations or Equation 4 to Equation 7

Notation used in which: A is cross-sectional area, a_v is pressure index, C_v is coefficient of consolida-tion, C_{vr} is radial consolidation coefficient, e_0 is initial void ratio, H is soil layer thickness, i is hydraulic gradient, k_h is soil horizontal permeability coefficient, k_v is soil vertical permeability coefficient, m_v is soil volume compression coefficient, q is water discharge, r_e is vertical drainage radius, S is surface settlement of soil, t is time, T is time factor, T_h is horizontal time factor, v is water velocity, V_i is volume of water at time i, γ_w is water weight unit, ΔH_w is changes in the water table, ΔV_w is change in water volume, σ_{pc} is preloading combination pressure, σ_v is vertical pressure, ΣV_i is total volume of water at time i

Derivation of the soil permeability equation as follows:

The basic equation: $q = vA = k_v i A$

and $i = \frac{\Delta H_w}{H}$, then $k_v = \frac{q H_s}{A \Delta H_w} = \frac{q H}{\Delta V_w}$

$q = \frac{k_v \Delta V_w}{H}$ or $k_v = \frac{qH}{\Delta V_w}$

The basic equation: $t = \frac{T_h r_e^2}{C_{vr}}$, and $t = \frac{T H^2}{C_v}$, then $C_{vr} = \frac{T_h r_e^2}{T H^2} C_v$

$T_h = \frac{t C_{vr}}{r_e^2}$ then $C_{vr} = \frac{t C_{vr}}{T H^2} C_v$, so that $\frac{t C_v}{T H^2} = 1$ or $t = \frac{T H^2}{C_v}$

$C_{vr} = \frac{k_h (1 + e_0)}{\gamma_w a_v}$ and $a_v = m_v(1 + e_0)$, $C_{vr} = \frac{k_h}{\gamma_w m_v}$, or $m_v \gamma_w = \frac{k_h}{C_{vr}}$

The basic equation: $S = H \sigma_v m_v$ or $m_v = \frac{S}{H \sigma_v}$

$\sigma_V = \sigma_{pc}$ so $m_v = \frac{S}{H \sigma_{pc}}$

$T = \frac{t C_v}{H^2}$, and $C_v = \frac{k_v}{\gamma_w m_v}$, then $T = \frac{t k_v}{\gamma_w m_v H^2} = \frac{t \frac{q H}{\Delta V_w}}{\gamma_w m_v H^2} = \frac{t q}{\gamma_w m_v H \Delta V_w}$

$T = \frac{t q}{\gamma_w m_v H \Delta V_w} = \frac{t q}{\gamma_w \frac{S}{H \sigma_v} H \Delta V_w} = \frac{t q \sigma_v}{\gamma_w S \Delta V_w}$

$T = \frac{t q_w \sigma_v}{\gamma_w S \Delta V_w} = \frac{V_i \sigma_v}{\gamma_w S \Sigma V_i}$

$C_{vr} = \frac{k_h H \sigma_v}{\gamma_w}$, or $\sigma_v = \frac{\gamma_w C_{vr}}{H k_h}$

$C_{vr} = \frac{T_h r_e^2}{T H^2}$ $C_v = \frac{T_h r_e^2}{T H^2} \frac{k_v}{\gamma_w m_v} = \frac{\frac{t C_{vr}}{r_e^2} r_e^2}{T H^2} \frac{k_v}{\gamma_w m_v} = \frac{t C_{vr}}{T H^2} \cdot \frac{k_v}{\gamma_w m_v}$

$\frac{t k_v}{H^2 \gamma_w m_v} = T$ so $k_v = \frac{T H^2 \gamma_w m_v}{t} = \frac{T H^2 \gamma_w \frac{S}{H \sigma_v}}{t} = \frac{T H \gamma_w S}{t \sigma_v}$

$k_v = \frac{T H \gamma_w S}{t \sigma_v} = \frac{\frac{t q}{\gamma_w m_v H \Delta V_w} H \gamma_w S}{t \sigma_v} = \frac{q S}{m_v \Delta V_w \sigma_v}$

$k_v = \frac{q S}{m_v \Delta V_w \sigma_v}$, and $m_v = \frac{q S}{k_v \Delta V_w \sigma_v}$

$T = \frac{t q}{\gamma_w m_v H \Delta V_w}$, or $m_v = \frac{t q}{\gamma_w T H \Delta V_w}$

$C_{vr} = \frac{k_h}{\gamma_w m_v} = \frac{k_h T H \Delta V_w}{t q}$

$C_{vr} = \frac{k_h T H \Delta V_w}{t q}$ if $k_h \approx k_v$, then $C_{vr} = \frac{k_v T H \Delta V_w}{t q}$

$C_{vr} = \frac{k_v T H \Delta V_w}{t q} = \frac{k_v T H \Delta V_w}{t \frac{k_v \Delta V_w}{H_s}} = \frac{T H^2}{t}$ this is because $k_h \approx k_v$, then $C_{vr} = C_v$

$T_h = \frac{t C_{vr}}{r_e^2} = \frac{k_v T H \Delta V_w}{q r_e^2}$

$k_v = \frac{q H_s}{A \Delta H_w}$, then $q = \frac{k_v \Delta V_w}{H_s}$

$T = \frac{qt}{\gamma_w m_v H \Delta V_w} = \frac{q t}{\gamma_w \frac{S}{H \sigma_v} H \Delta V_w} = \frac{q t \sigma_v}{\gamma_w S \Delta V_w}$

$T = \frac{q t \sigma_v}{\Delta V \gamma_w S} = \frac{\frac{k_v \Delta V_w}{H} t \sigma_v}{\Delta V \gamma_w S} = \frac{k_v \Delta V_w t \sigma_v}{\Delta V \gamma_w S H_s} = \frac{k_v t \sigma_v}{\gamma_w S H}$

$T = \frac{k_v t \sigma_v}{H \gamma_w S} = \frac{\frac{q H}{A \Delta H} t \sigma_v}{H \gamma_w S} = \frac{\frac{k_v \Delta V_w t \sigma_v}{H_s}}{\Delta V \gamma_w S} = \frac{k_v t \sigma_v}{\gamma_w S H}$

$k_v = \frac{T H \gamma_w S}{t \sigma_v} = \frac{T H \gamma_w S}{t \sigma_v} = \frac{\frac{q t \sigma_v}{A \Delta H \gamma_w S} H \gamma_w S}{t \sigma_v} = \frac{q H}{A \Delta H} = \frac{q H}{\Delta V}$

Derivation of the consolidation coefficient equation as follows:

$C_v = \frac{k_v}{\gamma_w m_v} = \frac{\frac{T H \gamma_w S}{t \sigma_v}}{\gamma_w m_v} = \frac{T H S}{t \sigma_v m_v} = \frac{T H S}{t \sigma_v \frac{S}{H \sigma_v}} = \frac{T H^2}{t}$

$C_v = \frac{k_v}{\gamma_w m_v} = \frac{k_v}{\gamma_w \frac{S}{H \sigma_v}} = \frac{k_v H \sigma_v}{\gamma_w S} = \frac{k_v H \sigma_{pc}}{S \gamma_w}$

Summary:

$k_v = \frac{q H_s}{\Delta V_w}$

$k_v = \frac{T H \gamma_w S}{t \sigma_{pc}}$

$T_h = \frac{k_r T H \Delta V_w}{q r_e^2}$

$m_v = \frac{S}{H \sigma_{pc}}$

if $k_h \approx k_v$ then $C_{vr} = \frac{k_r T H \Delta V_w}{t q}$

$T = \frac{k_v t \sigma_v}{H \gamma_w S}$

$T = \frac{V_i \sigma_{pc}}{\gamma_w S \Sigma V_i}$

$C_{vr} = \frac{k_v H \sigma_{pc}}{S \gamma_w}$

6.2. Dimensional Analysis for Equation 4 to Equation 7

1. Units of the time factor (T)

$$T = \frac{V_i \sigma_{pc}}{\gamma_w S \Sigma V_i} = \frac{\mathrm{m^3}\,\frac{\mathrm{kN}}{\mathrm{m^2}}}{\frac{\mathrm{kN}}{\mathrm{m^3}}\mathrm{m}\,\mathrm{m^3}} = \frac{\mathrm{m\,kN}}{\frac{\mathrm{kN}}{\mathrm{m^3}}\mathrm{m^4}} = \frac{\mathrm{m\,kN}}{\mathrm{m\,kN}} = 1, \text{ or without units}$$

Then the dimensionless time factor.

2. Unit of the soil permeability coefficient (k)

$$k = \frac{TS\gamma_w H}{t \sigma_{pc}} = \frac{(\text{without units})\,\mathrm{m}\,\frac{\mathrm{kN}}{\mathrm{m^3}}\,\mathrm{m}}{(\mathrm{Sec})\,\frac{\mathrm{kN}}{\mathrm{m^2}}} = \frac{\frac{\mathrm{kN}}{\mathrm{m}}}{(\mathrm{Sec})\,\frac{\mathrm{kN}}{\mathrm{m^2}}} = \frac{\frac{\mathrm{kN}}{\mathrm{m}}}{(\mathrm{Sec})\,\frac{\mathrm{kN}}{\mathrm{m}}\cdot\frac{1}{\mathrm{m}}} = \frac{1}{\frac{\mathrm{second}}{\mathrm{m}}} = \frac{\mathrm{m}}{\mathrm{sec}}$$

Then the soil permeability coefficient has unit length per unit time.

3. Unit of the coefficient of consolidation (C_v)

$$C_{vr} = \frac{k_v H \sigma_{pc}}{S \gamma_w} = \frac{\frac{\mathrm{m}}{\mathrm{sec}}\mathrm{m}\,\frac{\mathrm{kN}}{\mathrm{m^2}}}{\mathrm{m}\,\frac{\mathrm{kN}}{\mathrm{m^3}}} = \frac{\frac{\mathrm{kN}}{\mathrm{sec}}}{\frac{\mathrm{kN}}{\mathrm{m^2}}} = \frac{\mathrm{kN}}{\mathrm{sec}}\cdot\frac{\mathrm{m^2}}{\mathrm{kN}} = \frac{\mathrm{m^2}}{\mathrm{sec}}$$

Then the consolidation coefficient has units of length squared per unit time.

4. Unit of the coefficient of volume compression (m_v)

$$m_v = \frac{S}{H \sigma_{pc}} = \frac{\mathrm{m}}{\mathrm{m}\,\frac{\mathrm{kN}}{\mathrm{m^2}}} = \frac{1}{\frac{\mathrm{kN}}{\mathrm{m^2}}} = \frac{\mathrm{m^2}}{\mathrm{kN}}$$

Then the units of the coefficient of soil volume compression are length squared per unit force or cross-sectional area per unit force.

7. Declarations

7.1. Author Contributions

Conceptualization, E.S., S.P.R.W., and A.S.M.; methodology, E.S. and A.S.M.; validation, E.S., A.S.M., and S.P.R.W.; formal analysis, E.S.; investigation, E.S. and A.S.M.; resources, A.S.M.; data curation, E.S.; writing—original draft preparation, S.P.R.W.; writing—review and editing, S.P.R.W. and A.S.M.; visualization, E.S.; supervision, A.S.M.; project administration, A.S.M. All authors have read and agreed to the published version of the manuscript.

7.2. Data Availability Statement

The data presented in this study are available in the article.

7.3. Funding

This research was supported by PT. Teknindo Geosistem Unggul, a ground improvement specialist. The funding included the experiment equipments and publication.

7.4. Acknowledgements

I would like to express my deepest gratitude and appreciation to:

- Dr. Ilham Nurhuda, and Dr. Kresno Wikan, as examiner team Undip Semarang Indonesia.
- Dr. H.R.AR. Harry Anwar; Dr. Widjajani; and Prof. Hennie Husniah from Unla Bandung Indonesia for support, study funds, and research facilities.
- Ir. Wahyu Kuswanda as director of Teknindo Geosistem Unggul Company, Surabaya Indonesia, for support and research funds.
- Zulkarnaen, MT; Arkam, ST; and Jamal, ST as the electrical and informatics team from Bandung Indonesia.

7.5. Conflicts of Interest

The authors declare no conflict of interest.

8. References

[1] Kjellman, W. (1952). Consolidation of clay soil by means of atmospheric pressure. Proceedings of a Conference on Soil Stabilization, Massachusetts Institute of Technology, Massachusetts, United States.

[2] Suhendra, A., & Irsyam, M. (2011). Study of Vacuum Preloading Application as an Alternative Method to Accelerate the Consolidation Process on Water-saturated Soft Clay Soil: GVS Trial at Pantai Indah Kapuk Housing Complex, Jakarta. ComTech: Computer, Mathematics and Engineering Applications, 2(2), 1055. doi:10.21512/comtech.v2i2.2855.

[3] Li, L. H., Wang, Q., Wang, N. X., & Wang, J. P. (2009). Vacuum dewatering and horizontal drainage blankets: A method for layered soil reclamation. Bulletin of Engineering Geology and the Environment, 68(2), 277–285. doi:10.1007/s10064-009-0200-7.

[4] Lai, J., Li, P., Liu, W., & Tang, J. (2018). Visual Measurement Device and Experiment of Ground Water Level in Vacuum Preloading. Proceedings of GeoShanghai 2018 International Conference: Multi-Physics Processes in Soil Mechanics and Advances in Geotechnical Testing, 373–380. doi:10.1007/978-981-13-0095-0_42.

[5] Chu, J., Yan, S. W., & Yang, H. (2000). Soil improvement by the vacuum preloading method for an oil storage station. Geotechnique, 50(6), 625–632. doi:10.1680/geot.2000.50.6.625.

[6] Seah, T. H. (2006). Design and construction of ground improvement works at Suvarnabhumi Airport. Geotechnical Engineering Journal of the SEAGS & AGSSEA, 37, 171–188.

[7] Chu, J., Bo, M. W., & Choa, V. (2006). Improvement of ultra-soft soil using prefabricated vertical drains. Geotextiles and Geomembranes, 24(6), 339–348. doi:10.1016/j.geotexmem.2006.04.004.

[8] Mesri, G., & Khan, A. Q. (2011). Increase in shear strength due to vacuum preloading. 2011 Pan-Am CGS Geotechnical Conference, 2-6 October, 2011, Toronto, Canada.

[9] Mesri, G., & Khan, A. Q. (2012). Ground Improvement Using Vacuum Loading Together with Vertical Drains. Journal of Geotechnical and Geoenvironmental Engineering, 138(6), 680–689. doi:10.1061/(asce)gt.1943-5606.0000640.

[10] Long, P. V., Nguyen, L. V., Bergado, D. T., & Balasubramaniam, A. S. (2015). Performance of PVD improved soft ground using vacuum consolidation methods with and without airtight membrane. Geotextiles and Geomembranes, 43(6), 473–483. doi:10.1016/j.geotexmem.2015.05.007.

[11] Sun, L., Guo, W., Chu, J., Nie, W., Ren, Y., Yan, S., & Hou, J. (2017). A pilot test on a membraneless vacuum preloading method. Geotextiles and Geomembranes, 45(3), 142–148. doi:10.1016/j.geotexmem.2017.01.005.

[12] Cai, Y., Xie, Z., Wang, J., Wang, P., & Geng, X. (2018). New approach of vacuum preloading with booster prefabricated vertical drains (PVDs) to improve deep marine clay strata. Canadian Geotechnical Journal, 55(10), 1359-1371. doi:10.1139/cgj-2017-0412.

[13] Wang, P., Han, Y., Wang, J., Cai, Y., & Geng, X. (2019). Deformation characteristics of soil between prefabricated vertical drains under vacuum preloading. Geotextiles and Geomembranes, 47(6), 798–802. doi:10.1016/j.geotexmem.2019.103493.

[14] Kianfar, K., Indraratna, B., Rujikiatkamjorn, C., & Leroueil, S. (2015). Radial consolidation response upon the application and removal of vacuum and fill loading. Canadian Geotechnical Journal, 52(12), 2156–2162. doi:10.1139/cgj-2014-0511.

[15] Wang, J., Ma, J., Liu, F., Mi, W., Cai, Y., Fu, H., & Wang, P. (2016). Experimental study on the improvement of marine clay slurry by electroosmosis-vacuum preloading. Geotextiles and Geomembranes, 44(4), 615–622. doi:10.1016/j.geotexmem.2016.03.004.

[16] Xie, Z., Wang, J., Fu, H., Cai, Y., Xiuqing, H., Cai, Y., Zhang, Y., Ma, X., & Jin, H. (2019). Effect of pressurization positions on the consolidation of dredged slurry in air-booster vacuum preloading method. Marine Georesources & Geotechnology, 38(1), 122–131. doi:10.1080/1064119x.2018.1563252.

[17] Ke, S., Wang, P., Hu, X., Geng, X., Hai, J., Jin, J., Jiang, Z., Ye, Q., & Chen, Z. (2019). Effect of the pressurized duration on improving dredged slurry with air booster vacuum preloading. Marine Georesources & Geotechnology, 38(8), 970–979. doi:10.1080/1064119x.2019.1645250.

[18] Lei, H., Hu, Y., Zheng, G., Liu, J., Wang, L., & Liu, Y. (2019). Improved air-booster vacuum preloading method for newly dredged fills: Laboratory model study. Marine Georesources & Geotechnology, 38(4), 493–510. doi:10.1080/1064119x.2019.1599088.

[19] Anda, R., Fu, H., Wang, J., Lei, H., Hu, X., Ye, Q., Cai, Y., & Xie, Z. (2020). Effects of pressurizing timing on air booster vacuum consolidation of dredged slurry. Geotextiles and Geomembranes, 48(4), 491–503. doi:10.1016/j.geotexmem.2020.02.007.

[20] Shen, Y., Liu, Y., Geng, S., Qi, Y., Dong, S., Xin, X., Sun, J., & Zheng, H. (2021). Consolidation theory of homogeneous multilayer treatment by air-boosted vacuum preloading. European Journal of Environmental and Civil Engineering, 26(12), 5634–5652. doi:10.1080/19648189.2021.1915389.

[21] Feng, S., Lei, H., & Lin, C. (2022). Analysis of ground deformation development and settlement prediction by air-boosted vacuum preloading. Journal of Rock Mechanics and Geotechnical Engineering, 14(1), 272–288. doi:10.1016/j.jrmge.2021.05.006.

[22] Yao, K., Cheng, D., Sheng, J., Shi, L., Hu, L., & Yu, Y. (2023). Real-Time Behaviour of Dredged Slurry Treated by Air-Booster Vacuum Consolidation. Applied Sciences (Switzerland), 13(6), 3550. doi:10.3390/app13063550.

[23] Huangfu, Z., & Deng, A. (2024). Large strain consolidation model of vacuum and air-booster combined dewatering. Computers and Geotechnics, 171. doi:10.1016/j.compgeo.2024.106317.

[24] Gao, W., Han, L., Zhao, Y., Sun, J., & Liu, L. (2025). Consolidation analysis of soft ground with air-boosted vacuum preloading considering attenuation of vacuum and boost pressure. Scientific Reports, 15(1), 23161. doi:10.1038/s41598-025-04243-6.

[25] Sun, Y., Wang, F., Tang, Y., Yang, L., Chen, S., Du, Q., Huang, M., & Zhai, Q. (2025). Study on the effect and mechanism of hot-air-boosted vacuum preloading solidification of dredged silt via model tests. Applied Ocean Research, 161, 104684. doi:10.1016/j.apor.2025.104684.

[26] Zhang, H., Guo, L., & Tu, C. (2025). Experimental Investigation on the Improvement of Dredged Sludge Using Air–Booster Vacuum Preloading with Polyacrylamide Addition. Materials, 18(9), 2065. doi:10.3390/ma18092065.

[27] López-Acosta, N. P., Espinosa-Santiago, A. L., Pineda-Núñez, V. M., Ossa, A., Mendoza, M. J., Ovando-Shelley, E., & Botero, E. (2019). Performance of a test embankment on very soft clayey soil improved with drain-to-drain vacuum preloading technology. Geotextiles and Geomembranes, 47(5), 618–631. doi:10.1016/j.geotexmem.2019.103459.

[28] Zhu, D., Indraratna, B., Poulos, H., & Rujikiatkamjorn, C. (2020). Field study of pile–prefabricated vertical drain (PVD) interaction in soft clay. Canadian Geotechnical Journal, 57(3), 377-390.

[29] Sun, L., Gao, X., Zhuang, D., Guo, W., Hou, J., & Liu, X. (2018). Pilot tests on vacuum preloading method combined with short and long PVDs. Geotextiles and Geomembranes, 46(2), 243–250. doi:10.1016/j.geotexmem.2017.11.010.

[30] Chu, J., & Yan, S. W. (2005). Estimation of Degree of Consolidation for Vacuum Preloading Projects. International Journal of Geomechanics, 5(2), 158–165. doi:10.1061/(asce)1532-3641(2005)5:2(158).

[31] Chai, J. C., Carter, J. P., & Hayashi, S. (2005). Ground Deformation Induced by Vacuum Consolidation. Journal of Geotechnical and Geoenvironmental Engineering, 131(12), 1552–1561. doi:10.1061/(asce)1090-0241(2005)131:12(1552).

[32] Cai, Y., Qiao, H., Wang, J., Geng, X., Wang, P., & Cai, Y. (2017). Experimental tests on effect of deformed prefabricated vertical drains in dredged soil on consolidation via vacuum preloading. Engineering Geology, 222, 10–19. doi:10.1016/j.enggeo.2017.03.020.

[33] Indraratna, B., Rujikiatkamjorn, C., Baral, P., & Ameratunga, J. (2018). Performance of marine clay stabilised with vacuum pressure: Based on Queensland experience. Journal of Rock Mechanics and Geotechnical Engineering, 11(3), 598–611. doi:10.1016/j.jrmge.2018.11.002.

[34] Liu, J., Lei, H., Zheng, G., Zhou, H., & Zhang, X. (2017). Laboratory model study of newly deposited dredger fills using improved multiple-vacuum preloading technique. Journal of Rock Mechanics and Geotechnical Engineering, 9(5), 924–935. doi:10.1016/j.jrmge.2017.03.003.

[35] Yuan, X., Wang, Q., Lu, W., Zhang, W., Chen, H., & Zhang, Y. (2017). Indoor simulation test of step vacuum preloading for high-clay content dredger fill. Marine Georesources & Geotechnology, 36(1), 83–90. doi:10.1080/1064119x.2017.1285381.

[36] Fang, Y., Guo, L., & Huang, J. (2018). Mechanism test on inhomogeneity of dredged fill during vacuum preloading consolidation. Marine Georesources & Geotechnology, 37(8), 1007–1017. doi:10.1080/1064119x.2018.1522398.

[37] Li, J., Chen, H., Yuan, X., & Shan, W. (2020). Analysis of the effectiveness of the step vacuum preloading method: A case study on high clay content dredger fill in Tianjin, China. Journal of Marine Science and Engineering, 8(1), 38. doi:10.3390/JMSE8010038.

[38] Sakleshpur, V. A., Prezzi, M., & Salgado, R. (2018). Ground engineering using prefabricated vertical drains: A review. Geotechnical Engineering Journal of the SEAGS & AGSSEA, 49(1), 45-64.

[39] Aspara, W. A. N., & Fitriani, E. N. (2016). Effect of Distance and Pattern of Prefabricated Vertical Drain for Improvement of Soft Clay Soil. Majalah Ilmiah Pengkajian Industri, 10(1), 41-50. (In Indonesian).

[40] Panjaitan, S. R. N. (2020). Preloading Analysis with Prefabricated Vertical Drain (PVD) for Soft Soil Improvement in the Tebing Tinggi - Indrapura Toll Road Construction. Journal of Civil Engineering Building and Transportation, 4(2), 85-93. doi:10.31289/jcebt.v4i2.4161. (In Indonesian).

[41] Ngo, D. H., Horpibulsuk, S., Suddeepong, A., Hoy, M., Udomchai, A., Doncommul, P., Rachan, R., & Arulrajah, A. (2020). Consolidation behavior of dredged ultra-soft soil improved with prefabricated vertical drain at the Mae Moh mine, Thailand. Geotextiles and Geomembranes, 48(4), 561–571. doi:10.1016/j.geotexmem.2020.03.002.

[42] Berry Peter, L. (1987). An introduction TO Soil Mechanic. Mc Graw Hill Book Company, Columbus, United States.

[43] Sutarman, E. (2013). Concepts and Applications of Soil Mechanics. Penerbit Andi, Jogjakarta, Indonesia. (In Indonesian).

[44] Barron, R. A. (1948). Consolidation of Fine-Grained Soils by Drain Wells by Drain Wells. Transactions of the American Society of Civil Engineers, 113(1), 718–742. doi:10.1061/taceat.0006098.

[45] Sun, H., Wang, J., Wang, D., Yu, Y., & Wei, Z. (2020). Optimal design of plastic drainage boards for soft soil foundations considering uncertainties in soil parameters. Journal of Zhejiang University - Science A, 21(1), 15–28. doi:10.1631/jzus.a1900227. (In Chinese).

[46] Nghia, N. T., Lam, L. G., & Shukla, S. K. (2018). A New Approach to Solution for Partially Penetrated Prefabricated Vertical Drains. International Journal of Geosynthetics and Ground Engineering, 4(2), 11. doi:10.1007/s40891-018-0128-8.

[47] Nguyen, B. P., Yun, D. H., & Kim, Y. T. (2018). An equivalent plane strain model of PVD-improved soft deposit. Computers and Geotechnics, 103, 32–42. doi:10.1016/j.compgeo.2018.07.004.

[48] Qi, C., Li, R., Gan, F., Zhang, W., & Han, H. (2020). Measurement and Simulation on Consolidation Behaviour of Soft Foundation Improved with Prefabricated Vertical Drains. International Journal of Geosynthetics and Ground Engineering, 6(2), 23. doi:10.1007/s40891-020-00208-z.

[49] Wang, P., Han, Y., Zhou, Y., Wang, J., Cai, Y., Xu, F., & Pu, H. (2020). Apparent clogging effect in vacuum-induced consolidation of dredged soil with prefabricated vertical drains. Geotextiles and Geomembranes, 48(4), 524–531. doi:10.1016/j.geotexmem.2020.02.010.